Void structure and intermediate-range fluctuations in the metal-nonmetal transition range in expanded liquid Hg

Kenji Maruyama
Faculty of Science, Niigata University, Niigata 950-2181, Japan

Hirohisa Endo
Faculty of Science, Kyoto University, Kyoto 606-8224, Japan

Hideoki Hoshino
Faculty of Education, Hirosaki University, Hirosaki 036-8560, Japan

Friedrich Hensel
Physikalische Chemie, Philipps–Universität Marburg, 35032 Marburg, Germany

(Received 5 February 2009; revised manuscript received 18 March 2009; published 1 July 2009)

The reverse Monte Carlo and Voronoi-Delaunay analyses have been applied to characterize the intermediate-range fluctuations near the metal-nonmetal transition in expanded liquid Hg. An analysis of voids acts as a useful adjunct to the normally discussed structural properties in interpreting the origin of intermediate-range fluctuations in the expanded liquids. The results for Hg-based and void-based partial pair distribution functions and the partial coordination number distributions reveal that the metallic domains (M domains) are built with packing of tetrahedral Hg_4 blocks. The M domains transform into the nonmetallic domains (NM domains) creating large voids (L voids) ~3.1 Å in radius, which are supported by the network linked with tetrahedral Hg_4 blocks containing small voids (S voids) ~2.3 Å in radius at densities of 9.2–10.5 g cm^{-3}, where the coordination number is rapidly reduced below six. The estimated density variations in $S'_{cc}(0)$ from "domain model" and "void model" exhibit a peak around 10.5 g cm^{-3}, which indicates that M domains and NM domains coexist near the metal-nonmetal transition region. There appears the prepeak at 0.8–1.2 Å^{-1} in the partial structure factor of L voids around the L voids, $S'_{\text{LV-LV}}(Q)$, suggesting the chemical ordering of L voids. It follows that the intermediate-range concentration fluctuations resulting in microphase separation (clustering) of NM domains and M domains are reflected in the structural change near the metal-nonmetal transition.

DOI: 10.1103/PhysRevB.80.014201 PACS number(s): 61.20.−p, 61.25.Mv, 64.70.Ja

I. INTRODUCTION

During the past three decades, many experimental and theoretical investigations have been performed on the density variation in structural properties[1–7] of liquid (l-) Hg through large volume expansion up to liquid-gas critical point (the critical density[1] being d_c=5.8 g cm^{-3}). Much of effort has focused on the nearest-neighbor (NN) geometry of the structure[3,5–7] at the densities of 9–10 g cm^{-3} where the metal-nonmetal (M-NM) transition was proposed to occur.[8–13]

The x-ray diffraction experiments of l-Hg in the density range of 13.55–6.6 g cm^{-3} were made by Tamura and Hosokawa.[2] Their important results are that the volume expansion of l-Hg does result in a decrease in the average coordination number to about six near the M-NM transition region, while the mean interatomic distance remains roughly unchanged. The recent analysis by Inui *et al.*[3] revealed that the local structure of l-Hg is characterized by atoms coordinated at shorter distance of 3.0 Å and longer distance of 3.6 Å around a central atom, and Hg atoms are taken away from closer neighbors in the stage of volume expansion.

The results based on an *ab initio* density-functional molecular dynamics by Kresse and Hafner[5] show the formation of 6*s*-6*p* band gap at 8.8 g cm^{-3} and the presence of well-defined short-range correlations in a small cluster of a few atoms at the densities close to the M-NM transition.

The theoretical study by Kitamura[14] indicates that there appears the irregular mixing of high-density metallic domains (M domains) and low-density nonmetallic domains (NM domains) in the M-NM transition range and the time-scale of structural relaxation involving such a local M-NM transition is remarkably slow. Arai and McGreevy[6] applied reverse Monte Carlo (RMC) method[15] to x-ray diffraction data as provided by Tamura and Hosokawa.[2] They pointed out that the structure of expanded l-Hg contains atoms in a "semiconducting" environment and in a "metallic" environment, and the metallic bond network passes through a percolation transition[16] and ceases to be fully interconnected near the liquid-gas critical point.

The information regarding the intermediate-range order[4,17] beyond that of short-range order is indispensable for understanding the precise structural change near M-NM transition. It has been currently recognized that information regarding the distribution of voids[18–24] in liquids is of importance for interpreting the local structure of liquids in the intermediate scale. We will show that the distribution of the interstitial voids in expanded l-Hg is responsible for the atomic configurations in the intermediate scale near the M-NM transition region. In a previous paper[22] we applied RMC (Ref. 15) and Voronoi-Delaunay analyses[25,26] to characterize the chain geometries around voids in liquid Te.

In the present paper we present a distinct interpretation for the structural variation in l-Hg in the intermediate scale near the M-NM transition. RMC simulation and Voronoi-Delaunay analyses were performed on the basis of the structure factors S(Q) determined with x-ray diffraction experiments by Tamura and Hosokawa.[2] The relationship between the void distribution and M-NM transition is the subject of this paper.

II. METHOD

A. RMC analysis

The RMC method has been shown to be a useful tool[27] for extracting the three-dimensional (3D) structural aspects on the basis of diffraction data without knowledge of relevant interatomic potential.

The RMC analysis was performed on the basis of $S(Q)$ determined with energy-dispersive x-ray diffraction of l-Hg at 13.55–6.6 g cm^{-3} by Tamura and Hosokawa.[2] The standard RMC technique developed by McGreevy[15] was used to construct the three-dimensional structure model. A brief summary of the procedure is as follows. The number of atoms was 8000 and the length of an edge of a cubic box was about 60 or 70 Å. A distance of closest approach was set to be 2.0 Å. As starting configuration a fcc lattice was used. In the first step the position of atoms was statistically distributed. Then, the fittings were performed to minimize the residual errors of Q times $S(Q)$. After hundreds of accepted motions for each atom, an excellent agreement between the experimental data and RMC calculation was obtained. It should be noticed that we calculated the structure factor directly from the final configurations of RMC runs in order to rule out the possibility that the experimental $g(r)$ functions contain artifacts as a result of the Fourier transformation of the experimental structure factor $S(Q)$.

B. Void analysis

The radius of a circumsphere, which passes through the four atoms of the tetrahedron formed by bonding contiguous pairs of atoms gives a measure of empty space (void) in between the atoms, which is known as the Voronoi-Delaunay method.[25,26,28] We applied Voronoi-Delaunay method to the atomic configuration obtained by RMC in order to figure out the distribution of voids. As a result the center position and radius of circumsphere were obtained.

The set of voids derived from the analysis includes voids, which overlap each other.[25,28] In order to choose the set of voids of which the circumspheres do not overlap each other, the circumspheres were selected sequentially, starting from the largest radius discarding the voids of which the circumsphere overlapped one of the previously selected voids. Finally, the "nonoverlapped" sets of voids were obtained.

We used the radii of circumspheres as good indices of the size of nonoverlapping voids. We also determined the relative position of voids and atoms around the void in space by treating the circumspheres as the centers of spherical voids with the respective positions and calculated the partial pair distribution functions $g'_{ij}(r)$ for the voids as if they were particles with scattered radiation.

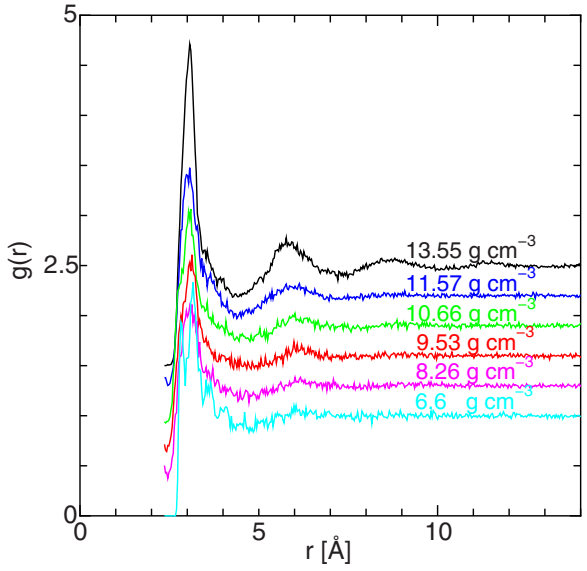

FIG. 1. (Color online) The pair distribution functions $g(r)$ of l-Hg at different densities obtained from RMC modeling.

III. RESULTS

Figure 1 shows the pair distribution functions $g(r)$ for l-Hg at different densities obtained from RMC simulation using Tamura and Hosokawa's $S(Q)$ results.[2] The first peak of $g(r)$ appears at 3.0 Å which is close to the NN distance in crystalline (c-)Hg.[29] There appears a shoulder at 3.6 Å behind the first peak corresponding to the Hg-Hg distance between the six next nearest neighbors in c-Hg. The third peak of $g(r)$ occurs at 5.8 Å at 13.55 g cm^{-3} and it shifts to 6.2 Å at lower densities.

We tried to fit the first peak and the shoulder of $g(r)$ using a simple method representing a series of Gaussian subshells up to 6 Å. The optimized first peak position r_S and shoulder position r_L, and the coordination number N_S around r_S and N_L around r_L are shown as a function of density in Fig. 2. The agreements between the present results and the earlier results by Inui *et al.*[3] are in general in good agreement, however, some differences are visible: r_S at 3.0 Å and r_L at 3.6 Å are kept at nearly constant, and slightly increase at the density below ~10 g cm^{-3}. N_S rapidly decreases with decreasing density, and reaches a value of about three at 10.26 g cm^{-3}. N_L remains unchanged down to ~11 g cm^{-3} and decreases rapidly to ~3 around 9 g cm^{-3}, which is suggestive of a structural transformation near the M-NM transition compared with the earlier results. The total coordination number N_S+N_L is ~6 around 9 g cm^{-3}.

Figures 3(a) and 3(b) show the "snapshot" of 5 Å-thick slice of a part of RMC configuration for l-Hg at 13.55 g cm^{-3} near the melting point and at 8.78 g cm^{-3} near the M-NM transition region. RMC configurations for l-Hg near the melting point indicate that the structure of l-Hg is built with the packing of edge-sharing or face-sharing tetrahedral Hg_4 blocks [Fig. 3(a)]. Near the M-NM transition re-

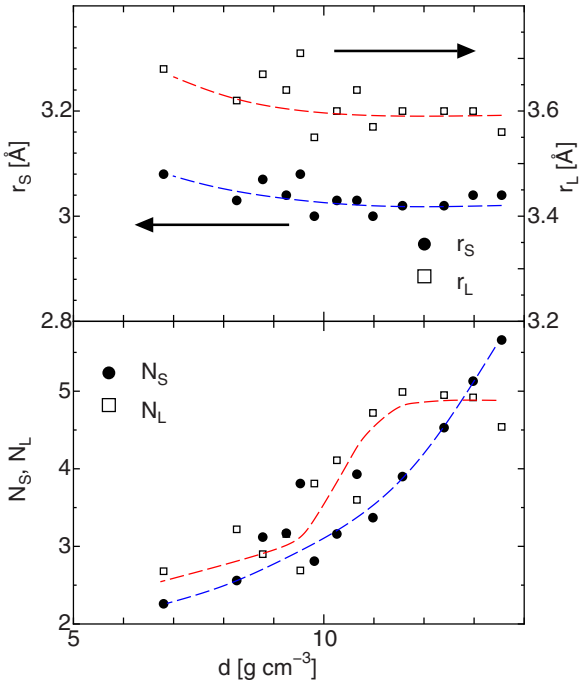

FIG. 2. (Color online) The positions of the optimized first peak and shoulder of $g(r)$, r_S, and r_L, and the optimized coordination number N_S located at r_S and N_L at r_L for l-Hg, respectively, as a function of density. The dashed lines are just a guide to eyes.

gion there appears a new environment in Hg atoms, where the network decorated by tetrahedral Hg_4 blocks supports voids as seen in Fig. 3(b) highlighted to show the distribution of the tetrahedral Hg_4 blocks and voids.

Figure 4 shows the Hg-Hg-Hg angular distribution $P(\theta)$ of l-Hg at 9.25 g cm^{-3} for the cutoff distances R_c=3.2 and 4.0 Å. A distinct peak at ~63° for R_c=3.2 Å corresponds to a vertical angle of Hg_4 block with an edge length of 3.0 Å. The preferred value at higher cutoff distance R_c=4.0 Å is ~56°, which is related to the angle between pairs of edges with lengths of 3.0 and 3.6 Å in the Hg_4 blocks. A broad peak around 110° is indicative of the bending angle between the neighbored tetrahedral Hg_4 blocks linked by corner sharing.

We estimated the tetrahedricity (T) of tetragonal Hg_4 blocks according to the definition[30]

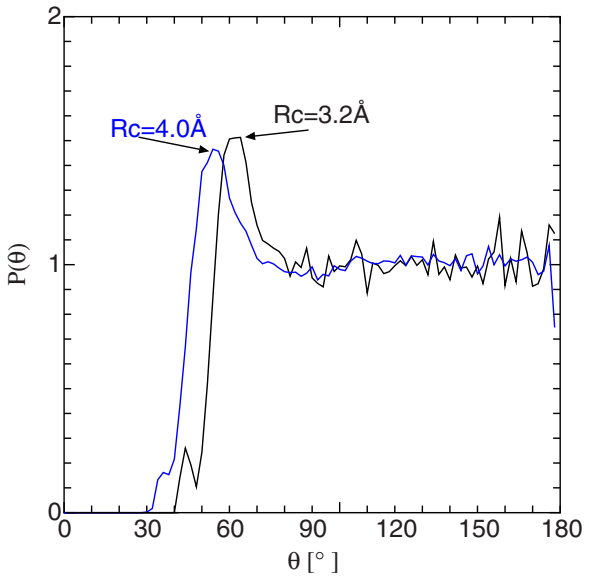

FIG. 4. (Color online) Hg-Hg-Hg angular distribution $P(\theta)$ of l-Hg at 9.25 g cm^{-3} for R_c=3.2 and 4.0 Å.

$$T = \sum_{j>i} \frac{(l_i - l_j)^2}{15\bar{l}^2}, \tag{1}$$

where l_i is the length of the ith tetrahedron edges and $\bar{l}^2$ is the average edge length. "Good" tetrahedron is characterized by values for $T \leq 0.016$.

From Fig. 5 it follows that a peak in the distribution of the tetrahedricity T lies at $T \sim 0.02$ for the density of 13.5 g cm^{-3} and the peak gradually shifts to higher T and becomes broad with long tail by lowering density. The peak of T lies at $T \sim 0.03$ at the density of 8.26 g cm^{-3}, where Hg-Hg bonds elongate. It seems to be clear that the tetrahedral Hg_4 blocks are comparatively stable even in the density range below M-NM transition. The results are coherent with our structural model.

Figures 6(a) and 6(b) show the partial coordination number distribution $P(N_{\text{Hg-Hg}})$ of Hg atoms around the Hg atom in l-Hg at 13.55, 9.53, and 8.26 g cm^{-3} for the cutoff distances R_c=3.3 Å and R_c=4.0 Å. The maximum in $P(N_{\text{Hg-Hg}})$ for R_c=3.3 Å appears at $N_{\text{Hg-Hg}}$=6–7 for

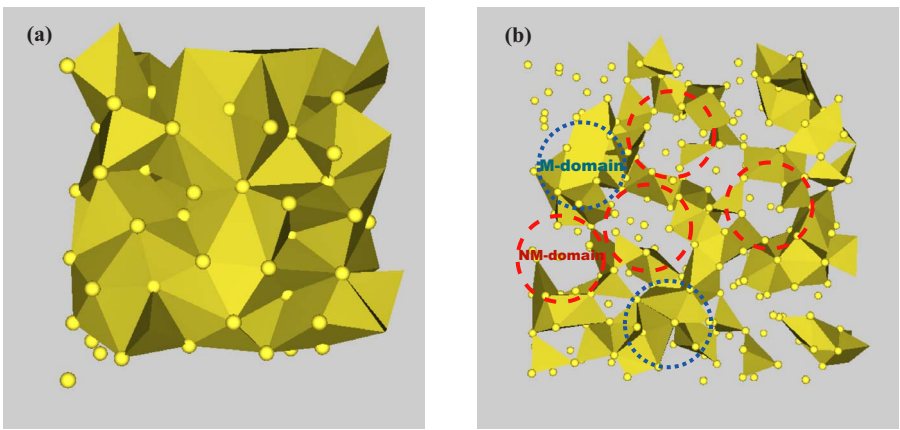

FIG. 3. (Color online) The RMC "snapshot" within a slice of 5 Å thick for the configuration of l-Hg at (a) 13.55 g cm^{-3} and at (b) 8.78 g cm^{-3}. The dotted and dashed circles represent M domains and NM domains, respectively, as described in the text (IV Discussion).

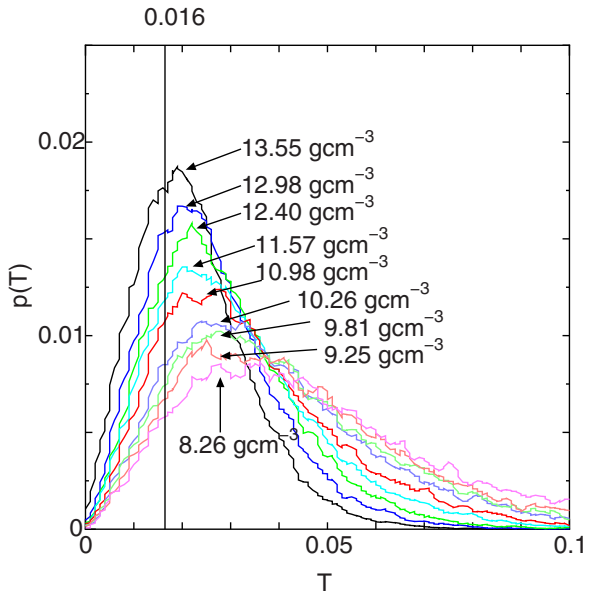

FIG. 5. (Color online) The distribution of tetrahedricity of Hg_4 blocks in the RMC configurations. The vertical line indicates the boundary for a "good" tetrahedron at T=0.016.

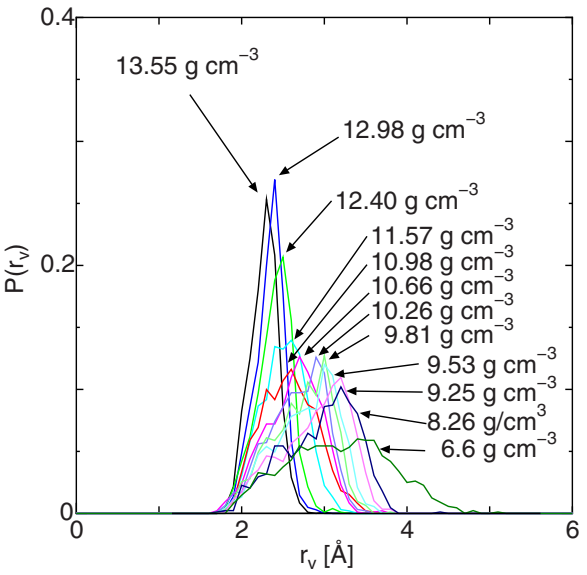

FIG. 7. (Color online) The size distribution of voids $P(r_V)$ at different densities in l-Hg as a function of radius r_V.

13.55 g cm^{-3} and $N_{Hg\text{-}Hg}$=3–4 for 9.53 and 8.26 g cm^{-3}. The large population at $N_{Hg\text{-}Hg}$=3–4 at lower densities where M-NM transition occurs, is suggestive of a strong preference of Hg atoms for the tetrahedral coordination. Hence the basic building block in expanded l-Hg can be considered as tetrahedral Hg_4 with the edge length of ~3.0 Å wherein three Hg atoms reside on the basal plane separated by ~3.6 Å. As seen in Fig. 6(b) $P(N_{Hg\text{-}Hg})$ gives a large population at $N_{Hg\text{-}Hg}$=6–7 for 9.53 and 8.26 g cm^{-3}, and $N_{Hg\text{-}Hg}$=11 for 13.55 g cm^{-3}, when R_c is increased to 4.0 Å. In considering the adjacent pairs of tetrahedral Hg_4 blocks interconnected at a common corner we get $N_{Hg\text{-}Hg}$ =2 at 3.0 Å and $N_{Hg\text{-}Hg}$=4 at 3.6 Å as the number of shared atoms around the corner (Cs site in Fig. 13).

Figure 7 shows the size distribution of voids $P(r_V)$ at different densities in l-Hg as a function of the radius of non-overlapping Delaunay circumsphere (see Sec. II). The figure is suggestive of two distinctive responses to a change in density. The distribution $P(r_V)$ has a well-defined peak at 2.3–2.4 Å in the higher density range near the melting point. This peak reduces substantially in intensity with decreasing density. At the same time an additional peak appears at the longer r range. At the density of 9.81 g cm^{-3} this can be clearly located at 3.1 Å while the peak at 2.3 Å is reduced to a shoulder in $P(r_V)$. Finally, at the density of 6.6 g cm^{-3} $P(r_V)$ becomes significantly broader. As a result we can postulate that the voids of l-Hg created in the stage of volume expansion at high temperature are not randomly distributed in size and there coexist small voids (S voids) ~2.3 Å in radius and large voids (L voids) ~3.1 Å in radius near M-NM transition region. The S void corresponds to the empty space inside of tetrahedral Hg_4 block.

The fractions of the number of S voids to L voids (non-overlapping) at different densities are shown in Fig. 8. The

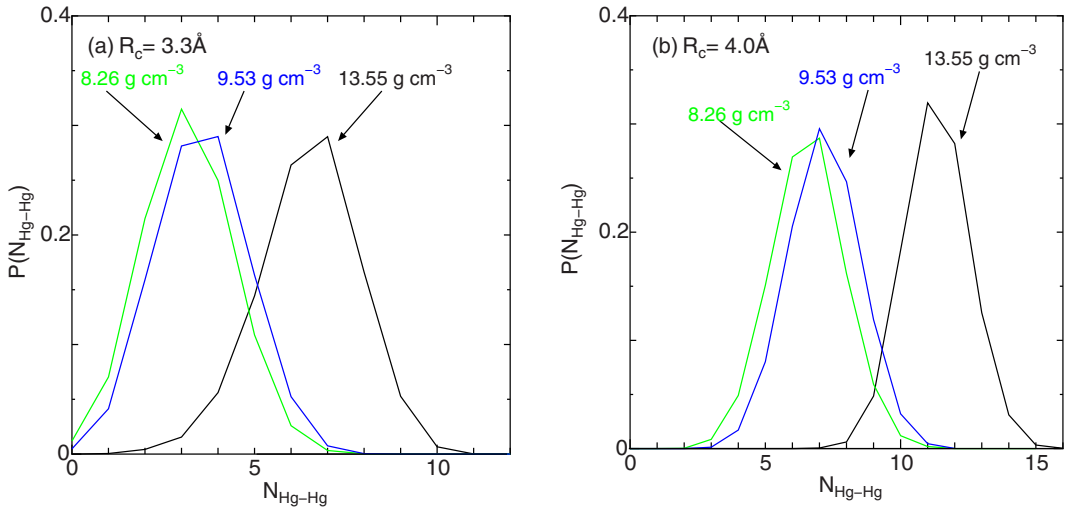

FIG. 6. (Color online) The coordination number distribution $P(N_{Hg\text{-}Hg})$ of Hg atoms around the Hg atom in l-Hg for 13.55, 9.53, and 8.26 g cm^{-3}, respectively, for the cutoff distances (a) R_c=3.3 Å and (b) R_c=4.0 Å.

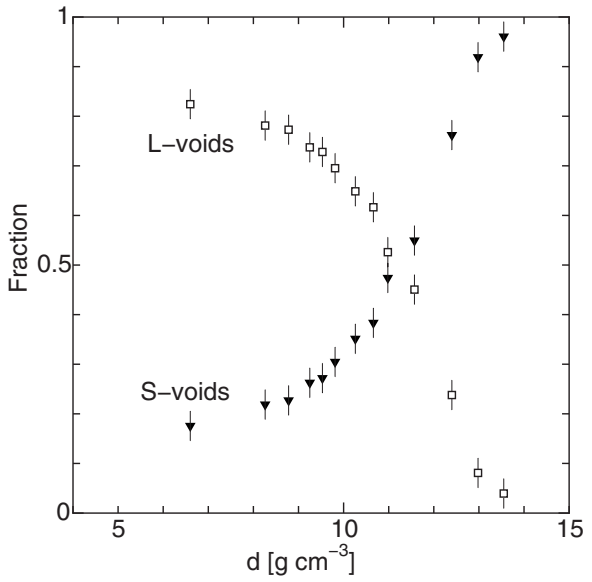

FIG. 8. The fractions of number of S voids ($r_V < 2.6$ Å) to L voids ($r_V \geq 2.6$ Å) as a function of density in l-Hg. Uncertainties are indicated by error bars.

fraction of S voids decreases with decreasing densities, while the fraction of L voids increases as seen in the figure. Of particular interest S voids are preserved down to much lower densities.

We have calculated the partial pair distribution functions of Hg atoms around the void, $g'_{V\text{-}Hg}(r)$, by treating the voids as if they were particles with scattered radiation. In Fig. 9 $g'_{V\text{-}Hg}(r)$ at different densities are shown. The sharp first peak of $g'_{V\text{-}Hg}(r)$ at 13.55 g cm^{-3} occurs at 2.3 Å, which coincides with the peak position of $P(r_V)$. The peak at 2.3 Å diminishes substantially with decreasing density and there appears an additional peak at the longer r range. In the low density the peak at the longer r range dominates the peak at

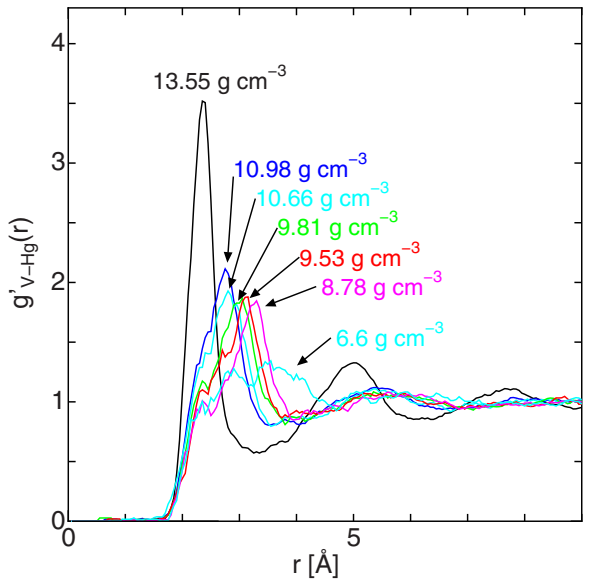

FIG. 9. (Color online) The partial pair distribution functions of Hg atoms around the void $g'_{V\text{-}Hg}(r)$ of l-Hg at different densities.

2.3 Å, corresponding to the radius of S void enclosed with the tetrahedral Hg_4 blocks, which is close to the radius estimated for the circumsphere passing through the four atoms of tetrahedron with an edge of 3.1 Å and a base of 3.6 Å. At 9.53 g cm^{-3} the peak is located at 3.1 Å and the shoulder persists at 2.3 Å. The peak corresponding to L void shifts to the higher r gradually with decreasing density. At 6.6 g cm^{-3} $g'_{V\text{-}Hg}(r)$ becomes less featured, which is indicative of the rapture of L voids.

The partial distribution functions of the relative positions between the center of S voids, $g'_{SV\text{-}SV}(r)$, at 9.53 g cm^{-3} and between the center of L voids, $g'_{LV\text{-}LV}(r)$, at 10.98, 10.66, 9.53, and 9.25 g cm^{-3} are shown in Figs. 10(a) and 10(b). The main peak of $g'_{SV\text{-}SV}(r)$ at 9.53 g m^{-3} splits into those at 5.5 and 6.2 Å and a small peak appears at 4.6 Å on the leading edge of the main peak. The $g'_{SV\text{-}SV}(r)$ curve in the longer r range contains a large statistical noise because of low concentration of S voids in this density range (see Fig. 8), however, the first minimum behind the main peak can be clearly recognized around 8.0 Å. The peak of $g'_{LV\text{-}LV}(r)$ at 9.53 g cm^{-3} is located at 6.2 Å, which is close to the distance between L void within the edge-linked hexagonal cage around L voids. Of particular interest the first peak shows characteristic narrowing at 9.53 g cm^{-3}, suggesting the clustering of L voids (microsegregation).

Figures 11(a) and 11(b) show the partial coordination number distribution $P(N_{SV\text{-}Hg})$ of Hg atoms around the S void and $P(N_{LV\text{-}Hg})$ of Hg atoms around the L void at different densities identified for $R_c = 3.1$ and 3.6 Å. As seen in Fig. 11(a), the preferred coordination number for $R_c = 3.1$ Å is $N_{SV\text{-}Hg} = 4$ at 9.53 and 8.26 g cm^{-3}, corresponding to the number of Hg atoms at vertices of the tetrahedron which contains the S void. The peak in $N_{SV\text{-}Hg} = 6$ at 13.55 g cm^{-3} is associated with six Hg atoms located at 3.0 Å around the central Hg atom. As seen in Fig. 11(b) $P(N_{LV\text{-}Hg})$ at 9.53 g cm^{-3} near the M-NM transition region for $R_c = 3.6$ Å suggests that a L void is surrounded by ~6 Hg atoms. The above evidence strongly supports that the local structure of expanded l-Hg comprises the hexagonal network decorated by tetrahedral Hg_4 blocks. The peak in $N_{LV\text{-}Hg}$ shifts to five at 8.26 g cm^{-3}, which implies that the connectivity of the tetrahedron-based network becomes loose as the density is lowered.

The partial coordination number $N_{LV\text{-}LV}$ distributions $P(N_{LV\text{-}LV})$ of L voids around the L void at various densities for $R_c = 10.0$ Å, which corresponds to the first minimum of $g'_{LV\text{-}LV}(r)$ are shown in Fig. 12. The results give a vivid picture of the degree of the connectivity of Hg_4 blocks network which supports L voids. The maximum in the $P(N_{LV\text{-}LV})$ at 10.66 g cm^{-3} appears at $N_{LV\text{-}LV} = 9$ and is shifted to $N_{LV\text{-}LV} = 10$ at 9.53 g cm^{-3} implying progressive clustering of L voids in the density range between 10.66 and 9.53 g cm^{-3}, and then conversely the maximum is shifted to lower value of $N_{LV\text{-}LV}$ below 9.25 g cm^{-3}, where the network relaxes with some bond breaking driven through the liquid-gas critical fluctuations. It is noticed that the average coordination number of L voids around the S void (inside of tetrahedral Hg_4 block) is ~3 at 9.53 g cm^{-3}, where the hexagonal networks are stabilized.

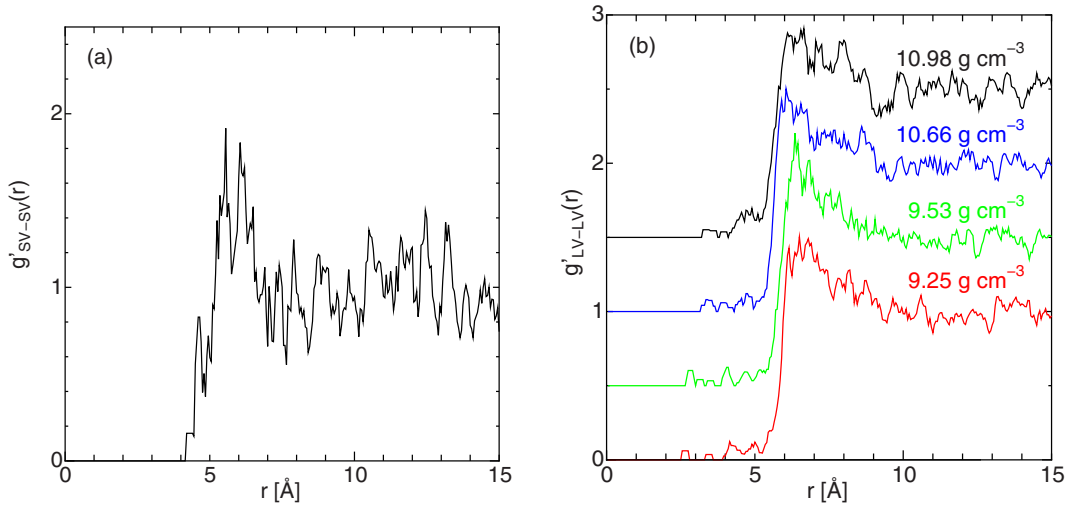

FIG. 10. (Color online) The partial distribution functions of (a) S voids, $g'_{\text{SV-SV}}(r)$ at 9.53 g cm^{-3} and (b) L voids, $g'_{\text{LV-LV}}(r)$ at 10.98, 10.66, 9.53, and 9.25 g cm^{-3}.

IV. DISCUSSION

Our "void model" based on the results for void-related $g'_{\text{LV-SV,LV}}(r)$, $P(N_{\text{LV-SV}})$, $P(\theta)$, etc., describes that the local structure of l-Hg in the metallic region can be envisaged in terms of an aggregate of structure motifs built with edge-sharing or face-sharing tetrahedral Hg_4 blocks (M domains) as indicated in Fig. 3(b) by dotted circles. Near the M-NM transition region there appear loosely packed nonmetallic domains containing L voids surrounded by corner-sharing tetrahedral Hg_4 blocks as indicated in Fig. 3(b) by dashed circles. It seems clear from this model that the volume expansion in which Hg-Hg distance remains unchanged while coordination numbers decrease, involves the formation of L voids which are defined in connectivity of tetrahedral Hg_4 blocks. Such a picture is very much coherent with the snapshot of characteristic configuration of Hg atoms in expanded l-Hg obtained by Kresse and Hafner.[5] Within this framework it may be taken as a firm evidence that there are still well-defined short-range correlations in a small cluster of a few Hg atoms (tetrahedral Hg_4 blocks) at much lower densities.

As shown in Fig. 13, a schematic illustration for the packing of voids and Hg atoms sketched in two-dimensional (2D) form allows us to understand the connectivity of the network and spatial distribution of L voids within the network. Notice that the spatial orientation of two neighbored Hg_4 tetrahedral blocks is not symmetric and the corner-linked hexagonal network is in general not planar.

Examination of the connectivity of S voids enclosed with tetrahedral Hg_4 blocks is a helpful way of characterizing M domains and NM domains arranged in a packing. The results for $g'_{\text{SV-SV}}(r)$ in Fig. 10(a) indicate that the NN distance between S voids which define the average separation of tetrahedral Hg_4 blocks is given to be 4.6 Å. The separations between the second-neighbored and third-neighbored S voids are given to be ~5.5 and ~6.2 Å, which meet the geometrical requirements for the hexagonal network of tetrahedral Hg_4 blocks involving L voids. It should be stressed here that

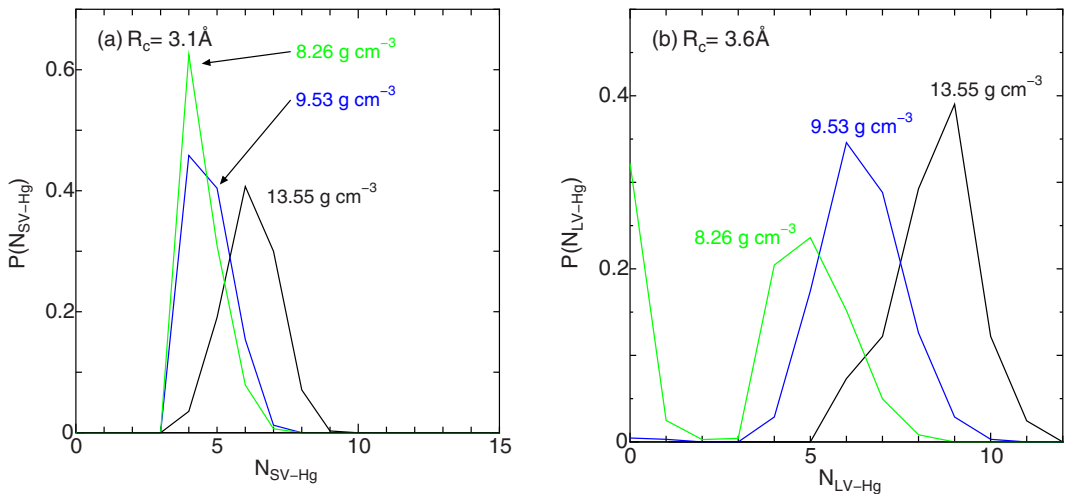

FIG. 11. (Color online) The coordination number distribution $P(N_{\text{SV-Hg}})$ of Hg atoms around the S void and $P(N_{\text{LV-Hg}})$ of Hg atoms around the L void at 13.55, 9.53, and 8.26 g cm^{-3}, respectively, for the cutoff distances (a) R_c=3.1 Å and (b) R_c=3.6 Å.

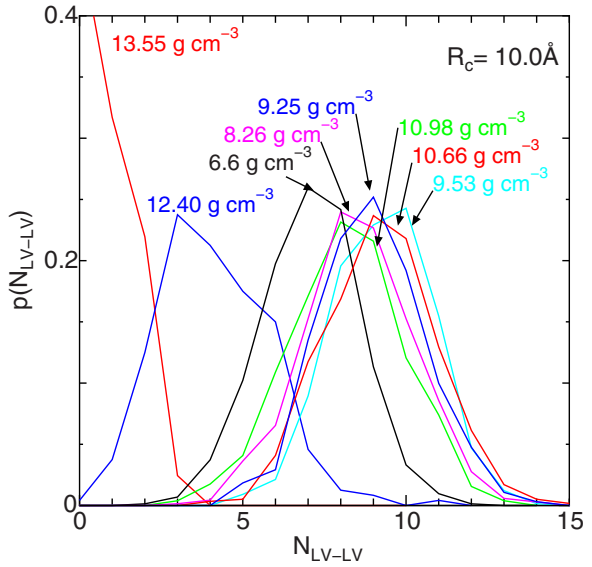

FIG. 12. (Color online) The coordination number distribution $P(N_{LV\text{-}LV})$ of L voids around the L void for R_c=10.0 Å at different densities.

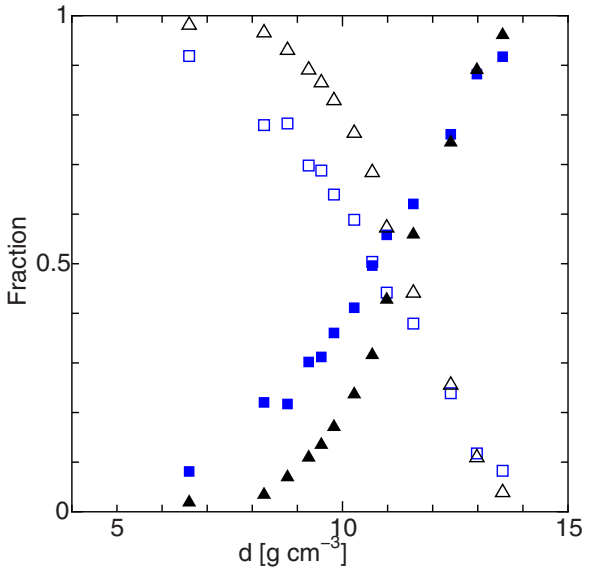

FIG. 14. (Color online) The fractions of the number of the M domains (▲) and the NM domains (△) as a function of density in l-Hg, together with those of M domains (■) and NM domains (□) obtained by Arai and McGreevy (Ref. 6).

the tetrahedral Hg_4 blocks linked by corner-sharing produce Hg_7 clusters, which comprise six coordinate sites [see Fig. 6(b)] centered at a common corner (C_S site in Fig. 13). The theoretical study on the structure of Hg clusters has been performed by Hartke *et al.*[31] They have predicted presence of a stable Hg_7 cluster of covalent character.

The presence of well-defined S voids and L voids gives a readily visualized measure related to the intermediate-range configurations of Hg atoms. As seen in Fig. 8 the number of S voids decreases linearly and rapidly with decreasing density, correspondingly the number of L voids increases. The number ratio of L voids to S voids is ~3 at 9.53 g cm^{-3}. Our void-related model confirms that the average coordination number of L voids around the S void (SV_c in Fig. 13) is ~3 in the M-NM transition region. Assuming that a few atoms in adjacent three M domains stay away from their atomic positions as indicated by dotted circles in Fig. 13, one L void supported by Hg_4 blocks is created.

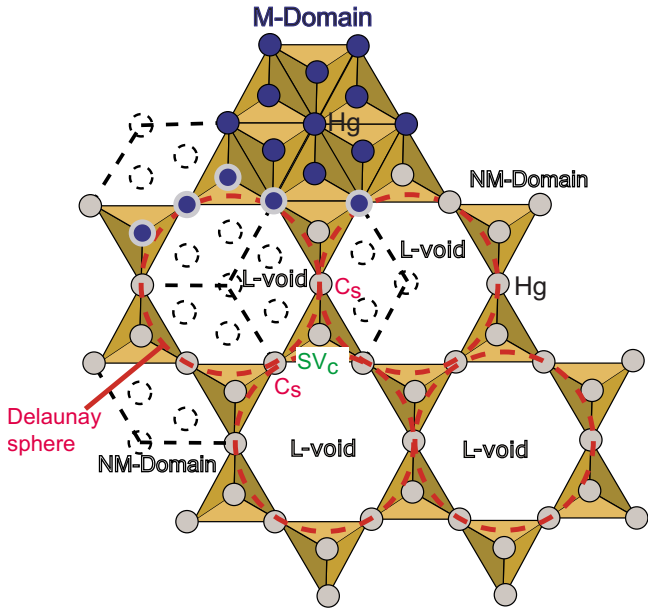

FIG. 13. (Color online) Schematic illustration in 2D for the packing of voids and Hg atoms. Here, the hexagonal cage around the L void is interconnected through a common corner. SVc and Cs represent the center of S void and the corner-linked site in a pair of the tetrahedral Hg_4 blocks. Dotted circles denote vacant sites in M domains created in the stage of volume expansion.

Following the above discussion, the fractions of the number of NM domains (open triangles) with coordination $N_{Hg\text{-}Hg} \leq 6$ within 3.6 Å to those of M domains (closed triangles) with higher coordination $N_{Hg\text{-}Hg} > 6$ within 3.6 Å are plotted as a function of density in Fig. 14. The figure indicates that the number fraction for M domains decreases rapidly as the density is lowered, while that for NM domains results in the concomitant increases in the magnitude of decrease in the number fraction for M domains. At lower densities than 10.5 g cm^{-3} the density variation in the fraction of M domains becomes slower. The coexistence of M domains and NM domains does not persist at the density of 8.26 g cm^{-3}. It is noteworthy that the curves for the number fraction of S voids and L voids as illustrated in Fig. 8 have similar density variations with those for M domains and NM domains in considering that six S voids (Hg_4 blocks) are captured around the L void in NM domains. This implies that the M-NM transition in an expanded l-Hg is controlled by the spatial distribution of L voids and S voids. The coexistence of M domains and NM domains near the M-NM transition range is consistent with the results for remarkably slow timescale (2 ns independent of density) in sound wave attenuation observed by Kohno and Yao,[32] which may be correlated with clustering of M domains and NM domains [see Figs. 10(b) and 12]. In Fig. 14 our results for the above "domain model" are compared with the analysis by Arai and

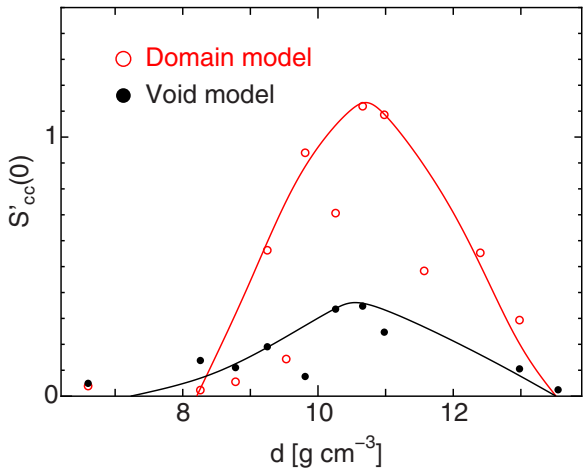

FIG. 15. (Color online) The density variation in $S'_{cc}(0)$ calculated for "domain model" and "void model" in l-Hg. The lines are just a guide to eyes.

McGreevy[6] in which they define the NM atoms in NM domains characterized by $N_{\text{Hg-Hg}}=3$ within 3.2 Å and the M atoms in M domains $N_{\text{Hg-Hg}}>3$ within 3.2 Å. They have proposed that the liquid-gas critical point may be related to the complete disappearance of the metallic cluster.

The concentration fluctuations $S_{cc}(0)$ corresponding to the long-wavelength limit of concentration-concentration structure factor $S_{cc}(Q)$ was calculated for both our "domain model" and "void model" using the partial distribution functions $g_{ij}(r)$ obtained from RMC configurations, by the formula as follows:[33]

$$S_{cc}(0) = c_i c_j [1 + \rho c_i c_j (G_{ij} + G_{jj} - 2G_{ij})], \tag{2}$$

with

$$G_{ij} = \int_0^\infty 4\pi r^2 [g_{ij}(r) - 1] dr, \tag{3}$$

where c_i and c_j denote concentration of M domains and NM domains or L voids and S voids, ρ denotes number density, and G_{ij} denote Kirkwood-Buff parameters,[34] which are given by Eq. (3). As shown in Fig. 15 the results for density variation of $S_{cc}(0)$ reveal that there exists a well-defined peak around 10.5 g cm^{-3} near the M-NM transition region for both "domain" and "void model," which suggests that the structural transformation near the M-NM transition region is accompanied by concentration fluctuations.

The covalently bonded hexagonal network of NM domains develops at the expense of M domains in a density range of 10.5–9.5 g cm^{-3} and the network relaxes with some bond breaking driven through the liquid-gas critical fluctuations by lowering density below 9.5 g cm^{-3}. The critical fluctuations obscure further development of the network with decreasing density. However, the extrapolations of the curve for the branches of M domains and NM domains in Fig. 14 to lower densities by the straight lines give the density in the final stage of structural transition to be about 9.2 g cm^{-3}. It should be stressed here that the progressive concentration fluctuations in the medium-ranged scale result in the microsegregation (clustering) of NM domains and M domains in the stage of volume expansion. In summary, our "void" analysis predicts that the M domains, densely packed by the tetrahedral Hg_4 blocks, transform at 10.5–9.2 g cm^{-3} into the hexagonal NM domains interconnected with the corner sharing of tetrahedral Hg_4 blocks around the empty space (L voids).

Recently Inui *et al.*[4] proposed that there appears the enhancement near the M-NM transition of the short-range correlation length, $R[=\xi(S(0)^{-1/2})]$, obtained from small angle x-ray scattering experiments, which is related to the second moment of Ornstein-Zernike direct correlation function, where ξ denotes correlation length of a density fluctuation and $S(0)$ fluctuations in a particle number. They have speculated in the framework of their results[4] that expanded l-Hg undergoes a first-order M-NM transition around 9 g cm^{-3}. However, their structural model does not provide reliable information on the geometrical configuration of Hg atoms in the intermediate-range scale. The enhancement of correlation length R near the M-NM transition can be understood in terms of the connectivity and packing in space of the tetrahedral Hg_4 blocks on the basis of our visualized structural model. The correlation length R is given to be 3 Å at 5 g cm^{-3} according to Ref. 4, which arises through the configuration defined by "isolated clusters" of tetrahedral Hg_4 blocks embedded in the continuous NM environment in our model. The correlation of Hg atoms on the covalently bonded networks linked with tetrahedral Hg_4 blocks which support L voids is expected to be ~6.2 Å (see Fig. 9) for R at 9–9.5 g cm^{-3}, where the microphase separation (clustering) of NM domains and M domains induced by concentration fluctuations occurs. At higher densities above 9.5 g cm^{-3}, the progressive growing of M domains and the consequent filling of L voids lead to reduction in the value of R, preventing the ordering of the L voids.

It is interesting to see if the low-Q features in the void-based structure factor $S'_{\text{SV-LV}}(Q)$ are associated with concentration fluctuations. Figure 16 shows the void-based partial structure factors $S'_{\text{LV-LV}}(Q)$, $S'_{\text{SV-LV}}(Q)$, and $S'_{\text{SV-SV}}(Q)$, together with the concentration-concentration structure factor $S'_{cc}(Q)/c_{\text{LV}}c_{\text{SV}}$ for expanded l-Hg (in Bhatia-Thornton formalism[35]) at 12.98 and 10.26 g cm^{-3}, where c_{LV} and c_{SV} are the concentrations of L voids and S voids in mole fraction.

The $S'_{\text{LV-LV}}(Q)$ at the density of 10.26 g cm^{-3} has a peak around 1.2 Å^{-1} corresponding to the distance between neighboring L voids within edge-linked hexagonal network of Hg_4 blocks. A slow rise near the leading edge in the first peak of $S'_{\text{LV-LV}}(Q)$ appears to be responsible for the correlation between L voids enclosed with corner-linked hexagonal network of Hg_4 blocks. The low-Q features of $S'_{\text{LV-LV}}(Q)$ are indicative of chemical ordering of L voids near the M-NM transition range.

The correlation between S voids and L voids provides information regarding the correlation between the tetrahedral Hg_4 blocks and L voids. The $S'_{\text{SV-LV}}(Q)$ has a minimum around 0.8 Å^{-1} which can be attributed to the distance (~8 Å) from the S void to the second-neighboring L void centers. The first peak of $S'_{\text{SV-LV}}(Q)$ at 1.2 Å^{-1} is assigned to the separation between the L void and tetrahedral Hg_4 block

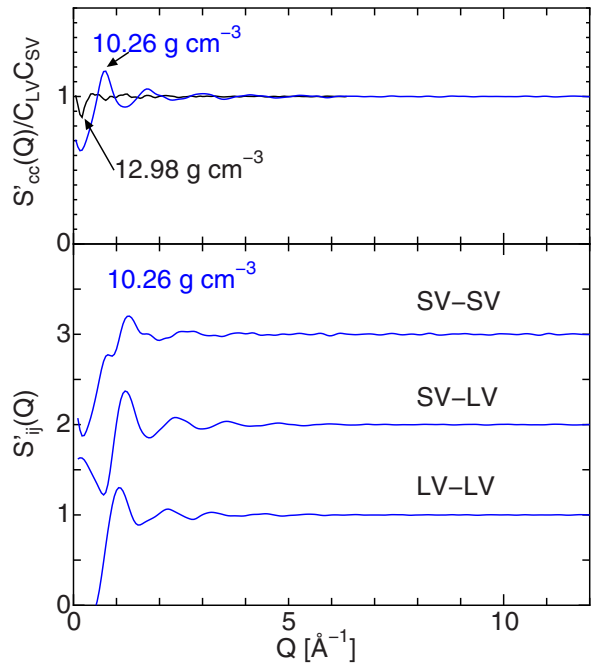

FIG. 16. (Color online) Partial structure factors $S'_{\text{LV-SV}}(Q)$, $S'_{\text{SV-SV}}(Q)$, and $S'_{\text{LV-LV}}(Q)$ in l-Hg at 10.26 g cm^{-3} produced from RMC configurations, together with the concentration-concentration structure factor $S'_{cc}(Q)/c_{\text{LV}}c_{\text{SV}}$ at 10.26 and 12.98 g cm^{-3}.

at the center of M domains. It is interesting to note here that the $S'_{\text{V-V}}(Q)$ in our previous work for l-$Rb_{20}Se_{80}$ (Ref. 23) composed of eight-membered Se rings has the prepeak around 1.0 Å^{-1}.

The peak in $S'_{\text{SV-SV}}(Q)$ around 1.2 Å^{-1} arises through the spatial correlation between pairs of S voids across the L voids, and the shoulder around 0.8 Å^{-1} through the second-neighbor distance of interconnected S voids. We see a well-defined prepeak at Q=0.8 Å^{-1} in $S'_{cc}(Q)/c_{\text{LV}}c_{\text{SV}}$ on the upper panel of Fig. 16.

These findings reveal that concentration fluctuations in the intermediate scale are significant in the structural transformation near the M-NM transition region, which results in the chemically ordered packing of M domains and NM domains. It is now understood that our "domain model" and "void model" are complementary to each other.

It should be noticed that the picture by Arai and McGreevy[6] in which is defined the percolating network of M domains in a NM domains surrounding in l-Hg near 10.5 g cm^{-3} is not capable of predicting the maximum in $S'_{cc}(0)$.

As seen in Fig. 14 the fraction of M domains is very small below 6.6 g cm^{-3}, where $g'_{\text{V-Hg}}(r)$ becomes less featured (see Fig. 9) suggesting rapture of connectivity of Hg_4 blocks around the L void. The density fluctuations which can be described by Ornstein-Zernike equation may become dominant in the vicinity of liquid-gas critical point below ~6.6 g cm^{-3}. Increase in intensity of $S(Q)$ in low-Q range may arise from the association of Hg_4 blocks or Hg_7 clusters. Consideration of this point awaits future work since only the numerical data of wide angle x-ray scattering down to 6.6 g cm^{-3} are available for us at the present stage.

V. CONCLUSION

The RMC and Voronoi-Delaunay analyses on expanded l-Hg at different densities were performed on the basis of the structure factors determined with x-ray diffraction experiments by Tamura and Hosokawa[2] to clarify the relationship between the void distribution and the structural transformation near the M-NM transition. The void analysis confirms that the structure of expanded l-Hg is represented as a binary mixture of M domains and NM domains. The M domains can be envisaged in terms of the packing of edge-shared or face-shared tetrahedral Hg_4 blocks, which enclose S voids, and loosely packed NM domains containing L voids surrounded by corner-shared tetrahedral Hg_4 blocks are created at lower densities. The estimated density variations in $S'_{cc}(0)$ from "domain model" and "void model" exhibit a peak around 10.5 g cm^{-3}, which indicates that M domains and NM domains coexist near the M-NM transition region. There appears the prepeak in $S'_{\text{LV-LV}}(Q)$ around 1.1 Å^{-1}, suggesting that M-NM transition arises through the chemical ordering of L voids (microsegregation of NM domains). These findings reveal that the intermediate-range concentration fluctuations resulting in the microphase separation (clustering) of NM and M domains are reflected in the structural change near the M-NM transition.

ACKNOWLEDGMENTS

This work was partly supported by a Grant-in-Aid for Scientific Research from the Ministry of Education, Science, Sport and Culture (MEXT), Japan (Grant No. 20540366) and by the University Education Internationalization Promotion Program of MEXT. One of the authors (K.M.) is grateful to F. Hensel and W.-C. Pilgrim for their encouragement and hospitality during his stay in Marburg University.

[1] F. Hensel and W. W. Warren, Jr., *Fluid Metals* (Princeton University, Princeton, NJ, 1999).
[2] K. Tamura and S. Hosokawa, Phys. Rev. B **58**, 9030 (1998).
[3] M. Inui, X. Hong, and K. Tamura, Phys. Rev. B **68**, 094108 (2003).
[4] M. Inui, K. Matsuda, D. Ishikawa, K. Tamura, and Y. Ohishi, Phys. Rev. Lett. **98**, 185504 (2007).
[5] G. Kresse and J. Hafner, Phys. Rev. B **55**, 7539 (1997).
[6] T. Arai and R. L. McGreevy, J. Phys.: Condens. Matter **10**, 9221 (1998).
[7] V. M. Nield and P. T. Verronen, J. Phys.: Condens. Matter **10**, 8147 (1998).
[8] F. Hensel and E. U. Franck, Rev. Mod. Phys. **40**, 697 (1968).
[9] K. Tsuji, M. Yao, and H. Endo, J. Phys. Soc. Jpn. **42**, 1594

(1977).
[10] M. Yao and H. Endo, J. Phys. Soc. Jpn. **51**, 966 (1982).
[11] L. F. Mattheiss and W. W. Warren, Jr., Phys. Rev. B **16**, 624 (1977).
[12] J. R. Franz, Phys. Rev. Lett. **57**, 889 (1986).
[13] N. F. Mott, Philos. Mag. **24**, 1 (1971).
[14] H. Kitamura, J. Phys.: Condens. Matter **15**, 6427 (2003).
[15] R. L. McGreevy, J. Phys.: Condens. Matter **13**, R877 (2001).
[16] I. Webman, J. Jortner, and M. H. Cohen, Phys. Rev. B **11**, 2885 (1975).
[17] M. J. Swenson and L. Börjesson, J. Non-Cryst. Solids **223**, 223 (1998).
[18] S. R. Elliott, J. Phys.: Condens. Matter **4**, 7661 (1992).
[19] V. P. Voloshin, S. Beaufils, and N. N. Medvedev, J. Mol. Liq. **96-97**, 101 (2002).
[20] W. Hoyer, R. Kleinhempel, A. Lörinczi, A. Pohlers, M. Popescu, and F. Sava, J. Phys.: Condens. Matter **17**, S31 (2005).
[21] M. Wilson, P. A. Madden, N. N. Medvedev, A. Geiger, and A. Appelhagen, J. Chem. Soc., Faraday Trans. **94**, 1221 (1998).
[22] K. Maruyama, H. Endo, and H. Hoshino, J. Phys. Soc. Jpn. **77**, 034603 (2008).
[23] K. Maruyama, H. Endo, and H. Hoshino, J. Phys. Soc. Jpn. **74**, 3213 (2005).
[24] K. Maruyama, H. Endo, and H. Hoshino, J. Phys. Soc. Jpn. **76**, 024601 (2007).
[25] S. L. Chan and S. R. Elliott, Phys. Rev. B **43**, 4423 (1991).
[26] Y. Hiwatari, T. Saito, and A. Ueda, J. Chem. Phys. **81**, 6044 (1984).
[27] X. Hong, J. Non-Cryst. Solids **353**, 3399 (2007).
[28] A. G. Vorontsov, A. A. Milzoev, and G. P. Vyatkin, J. Non-Cryst. Solids **353**, 3510 (2007).
[29] J. Donohue, *Structure of the Elements* (Wiley, New York, 1974), p. 231.
[30] N. N. Medvedev, A. Geiger, and W. Brostow, J. Chem. Phys. **93**, 8337 (1990).
[31] B. Hartke, H.-J. Flad, and M. Dolg, Phys. Chem. Chem. Phys. **3**, 5121 (2001).
[32] H. Kohno and M. Yao, J. Phys.: Condens. Matter **13**, 10293 (2001).
[33] M. Misawa and K. Yoshida, J. Phys. Soc. Jpn. **69**, 3308 (2000).
[34] J. G. Kirkwood and F. P. Buff, J. Chem. Phys. **19**, 774 (1951).
[35] A. B. Bhatia and D. E. Thornton, Phys. Rev. B **2**, 3004 (1970).